

pubs.acs.org/JCTC Review

Exploring Locality in Molecular Dirac-Coulomb-Breit Calculations: A Perspective

Can Liao, Eleftherios Lambros, Qiming Sun, Kenneth G. Dyall, and Xiaosong Li*



Cite This: J. Chem. Theory Comput. 2023, 19, 9009–9017



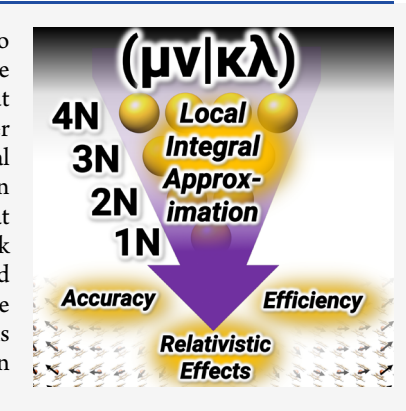
ACCESS I

III Metrics & More

Article Recommendations

s Supporting Information

ABSTRACT: The Dirac-Coulomb-Breit (DCB) operator is widely recognized for its ability to accurately capture relativistic effects and spin-physics in molecular calculations. However, due to its high computational cost, there is a need to develop low-scaling approximations without compromising accuracy. To tackle this challenge, it becomes essential to gain a deeper understanding of the DCB operator's behavior. This work aims to explore local integral approximations, shedding light on the locality of the parts of the charge-current distribution due to the small component. In particular, we propose an atomic Breit approximation that leverages an analysis of the behavior observed in a series of gold chains. Through benchmark studies of metal complexes, we evaluated the accuracy and performance of the proposed atomic Breit approximation. This work provides a comprehensive understanding of the behavior of the charge-current distribution in terms of its contributions from its AO basis constituents, facilitating the development of low-scaling methods that strike a balance between computational efficiency and accuracy.



1. INTRODUCTION

The Dirac-Coulomb-Breit (DCB) operator, derived from quantum field theory with the instantaneous electron—electron interaction, provides the most accurate description^{1–12} of electron—electron interactions before going to a genuine relativistic quantum field representation of many-electron systems. This operator accounts for important relativistic effects such as scalar relativity and spin-own-orbit, spin-other-orbit, spin-spin, and orbit-orbit interactions.

The Dirac-Coulomb-Breit operator in the Coulomb gauge includes the Coulomb, Gaunt (magnetic), and gauge interactions, ²⁴

$$V(r_{ij}) = \frac{1}{r_{ij}} - \frac{1}{2} \left(\frac{\boldsymbol{\alpha}_i \cdot \boldsymbol{\alpha}_j}{r_{ij}} + \frac{\boldsymbol{\alpha}_i \cdot \mathbf{r}_{ij} \boldsymbol{\alpha}_j \cdot \mathbf{r}_{ij}}{r_{ij}^3} \right), \quad \boldsymbol{\alpha}_{i,q} = \begin{pmatrix} \mathbf{0}_2 & \sigma_q \\ \sigma_q & \mathbf{0}_2 \end{pmatrix},$$

$$q = \{x, y, z\}$$

where $\{i, j\}$ are electron indices and $\mathbf{0}_2$ is the 2×2 zero matrix. The components of the Pauli matrices $\boldsymbol{\sigma}$ matrices are defined as

$$\sigma_{x} = \begin{pmatrix} 0 & 1 \\ 1 & 0 \end{pmatrix}, \quad \sigma_{y} = \begin{pmatrix} 0 & -i \\ i & 0 \end{pmatrix}, \quad \sigma_{z} = \begin{pmatrix} 1 & 0 \\ 0 & -1 \end{pmatrix}$$
 (2)

The high computational cost of the relativistic integrals is usually the limiting factor for the practical application of the Dirac-Coulomb-Breit operator in molecular calculations. The use of three-center density-fitting integrals partially mitigates this issue in an in-core algorithm but is still bound by the size of memory. ^{25,26} In a different vein, spin separation ^{22,23,27} of the Dirac Hamiltonian using the restricted kinetic balance (RKB)

condition and the Dirac identity can separate the DCB operator into scalar and spin- and orbit-dependent parts, with the scalar relativity capturing the majority of the electron—electron interaction.²⁸ The full spin-separation of the Dirac-Coulomb-Breit Hamiltonian has recently been implemented using the Pauli quaternion basis with the RKB condition.^{22,23} The realization of the scalar formalism of the DCB operator further reduces the computational cost of building the zero-order relativistic Hamiltonian.²⁸ Electronic structure methods that use only the scalar part of the Hamiltonian are of a lower computational cost than the full DCB operator because the scalar relativistic effects need only a fraction of the relativistic integrals. However, scalar relativistic Hamiltonians lack important spin-dependent terms, such as spin—orbit and spin—spin interactions.

In Equation 1, the Dirac matrices in the Breit operator connect the large and small components for each electron, and hence, the integrals for this operator contain two small component functions. These are (LSILS) type integrals; we distinguish the Gaunt and gauge integrals in what follows. The small component is localized near the atomic nuclei, so any density that contains a small component function is also localized on the nuclei. Thus, approximations with only the LS

Received: September 14, 2023 Revised: November 13, 2023 Accepted: November 15, 2023

Published: December 13, 2023





or SS densities that are localized on atomic centers are likely to be good approximations.

We can also gain some understanding of why this is so from the point of view of the operators in the modified Dirac representation. The use of RKB to generate the small component basis introduces a momentum operator ${\bf p}$ for each small component basis function. Consequently, the integrals, now taken over the large component basis, involve modified two-electron operators. Since ${\bf p}$ scales as 1/r, the modified Breit operator in these integrals scales as r^{-3} . A similar modification to the operator is introduced by RKB for the Coulomb terms that involve the small component: the modified operator for the (LLISS) integrals scales as r^{-3} and for the (SSISS) integrals, it scales as r^{-5} . Practically speaking, the integrals are evaluated as derivatives of various orders of the (LLILL) integrals.

Time-reversal symmetry also plays a role in the Breit interaction, as the direct contributions to the Breit energy cancel when summed over Kramers partners (see ref 29 for example). Only the exchange contribution remains for closed-shell systems and systems with a single unpaired electron. If unrestricted SCF methods are used, the cancellation is almost but not quite complete.

The goal of this work is to propose a strategy to lower the computational cost of calculations with the DCB operator based on the locality of the small component. We will explore several local integral approximations, aiming to provide a comprehensive understanding of the locality of the contributions arising from different modified relativistic operators and to aid in the development of low-scaling DCB methods without a significant loss of spin physics.

2. LOCAL RELATIVISTIC INTEGRAL APPROXIMATIONS

The following notation will be used unless otherwise specified:

- μ , ν , λ , κ : large component atomic orbitals (AOs).
- μ' , ν' , λ' , κ' : first-derivative of atomic orbitals (AOs). In the context of the restricted-kinetic-balance (RKB) condition ($\mu^S = \frac{1}{2c} \boldsymbol{\sigma} \cdot \mathbf{p} \mu^L$), the first-derivative of an AO is related to the small component basis.
- A, B: atomic center index.

The full spin-separation of the DCB operator offers a unique opportunity to explore the integral locality and its importance in relativistic Hamiltonians. For the spin-separated Dirac-Coulomb Hamiltonian under the restricted kinetic balance (RKB) conditions in the Pauli quaternion representation, 22,23 scalar integrals of the form $(\mu\nu l\kappa'\lambda')$ and $(\mu'\nu'l\kappa'\lambda')$ in Mulliken notation are used in the full Hamiltonian build. The spin-separated Breit Hamiltonian uses relativistic scalar integrals of the form $(\mu'\nu l\kappa'\lambda)$ and $(\mu'\nu l\kappa'\lambda)_3,^{22,23}$ where the subscript "3" denotes the $|{\bf r}_{12}|^{-3}$ operator for the gauge integral. 23

2.1. Atomic One-Center Approximation. The atomic one-center (A1N) approximation explores the extreme local limit of the Dirac-Coulomb-Breit contributions to the Fock matrix, where relativistic integrals are computed if and only if all four basis functions are localized on the same atom (the (AAIAA) type integrals). Functionally this means that the DCB operator is represented in an atomic block-diagonal form. In this scheme, the individual components of the DCB operator are expressed as

```
(LLISS): (\mu\nu |\kappa'\lambda')
(SSISS): (\mu'\nu' |\kappa'\lambda')
Gaunt or (LSILS): (\mu'\nu |\kappa'\lambda)
gauge or (LSILS)<sub>3</sub>: (\mu'\nu |\kappa'\lambda)_3
when \mu, \nu, \kappa, \lambda \in A
```

Note that the Dirac-Coulomb contribution is separated into the $O(c^0)$ order (LLILL), $O(c^{-2})$ order (LLISS), and $O(c^{-4})$ order (SSISS) terms. The (LLILL) term represents the classical Coulombic interaction between large components and is kept in its exact form without any local approximation.

The A1N approximation is similar to the atomic mean-field (AMF) interaction where only electron—electron interactions localized on the same atom are considered. However, because the A1N approximation is performed on the atomic integrals directly, it can be used in variational calculations in which the quaternion densities are fully optimized. This is in contrast to the AMF interaction, which uses the atomic DCB Hamiltonian as a frozen perturbation on the system.

The A1N approximation for the relativistic integrals also scales linearly with the number of atoms in the system, since all terms that span multiple atoms are neglected. If a system has multiple identical atoms, then the integrals for only one of those atoms need to be calculated. This reduces the amount of computation and memory needed for the formation of the Fock matrix at the start of each SCF procedure. It is also emphasized that the A1N approximation still formally includes two-electron interactions but is limited to those localized on the same atom.

2.2. Atomic Two-Center Approximation. The atomic two-center (A2N) approximation extends the A1N approximation by allowing the inclusion of integrals whose basis functions are centered on up to two separate atoms but where the basis functions for a given electron are always on the same atom. Thus, it includes (AAlBB) type integrals but not (AAl AB) or (ABlAB) type integrals, where A and B represent atomic centers. This pushes the approximation to a slightly less local regime where the additional individual DCB terms are computed as follows:

```
(LLISS): (\mu\nu |\kappa'\lambda')

(SSISS): (\mu'\nu' |\kappa'\lambda')

Gaunt or (LSILS): (\mu'\nu |\kappa'\lambda)

gauge or (LSILS)<sub>3</sub>: (\mu'\nu |\kappa'\lambda)_3

when \mu, \nu \in \{A\}; \kappa, \lambda \in \{B\}
```

While it is still a local integral approximation, the A2N approach includes interatomic interactions between pairs of atoms. This choice results in a quadratic scaling method, with respect to the number of atoms in the system.

2.3. Local Small-Component Approximations. The atomic approximations detailed in the preceding sections are designed to explore the atomic character of the relativistic integrals. As highlighted in the Introduction, given that the small component is primarily localized around the atomic nuclei, a viable strategy involves constraining integrals according to the locality of the small component. Herein, two local small-component approximations are proposed that

include relativistic integrals only if two small component basis functions are localized on the same atom.

The first local small-component approximation considers integrals with basis functions centered on a maximum of two distinct atoms. We will refer to this type of local approximation as SS2N, which is formally defined as

(LLISS):
$$(\mu\nu \kappa'\lambda')$$
 when $\mu, \nu \in \{A, B\}; \kappa, \lambda \in \{B\}$
(SSISS): $(\mu'\nu'\kappa'\lambda')$ when $\mu, \nu, \kappa, \lambda \in \{A, B\}$
Gaunt: $(\mu'\nu \kappa'\lambda)$ when $\nu, \lambda \in \{A, B\}; \mu, \kappa \in \{B\}$
gauge: $(\mu'\nu \kappa'\lambda)_3$ when $\nu, \lambda \in \{A, B\}; \mu, \kappa \in \{B\}$

In the (SSISS) term, the SS2N approach is more permissive than the A2N approximation, as it includes additional integrals, such as the (ABIAB) and (AAIAB) types.

The SS2N approximation can be broadened to a more inclusive model, termed SS3N, including the computation of integrals where the large component functions span up to three atomic centers:

```
 \begin{array}{ll} \text{(LLISS):} \; (\mu\nu | \kappa'\lambda') & \text{when } \mu, \; \nu \in \{A, B, C\}; \; \kappa, \; \lambda \in \{B\} \\ \text{(SSISS):} \; (\mu'\nu' | \kappa'\lambda') & \text{when } \mu, \; \nu, \; \kappa, \; \lambda \in \{A, B, C\} \\ \text{Gaunt or (LSILS):} \; (\mu'\nu | \kappa'\lambda) & \text{when } \nu, \; \lambda \in \{A, B, C\}; \; \mu, \; \kappa \in \{B\} \\ \text{gauge or (LSILS)_3:} \; (\mu'\nu | \kappa'\lambda)_3 & \text{when } \nu, \; \lambda \in \{A, B, C\}; \; \mu, \; \kappa \in \{B\} \\ \end{array}
```

For the (SSISS) term, the SS3N approach adds additional integrals, such as the (AAIBC) and (ABIAC) types.

3. RESULTS AND DISCUSSION

3.1. Computational Details. All calculations in this work are performed with a development version of the Chronus

Table 1. Ground State Energy Contributions (in au) from the (LLISS), (SSISS), Gaunt, and Gauge Terms of the DCB Operator (see Supporting Information for SCF Energies Used in This Analysis)^a

	$\Delta E_{ m full}^{ m (LLISS)}$	$\Delta E_{ m full}^{ m (SSISS)}$	$\Delta E_{ m full}^{ m Gaunt}$	$\Delta E_{ m full}^{ m gauge}$
Au_2	397.67	4.59	24.17	19.05
Au_4	833.26	9.30	48.35	38.09
Au_6	1285.64	14.06	72.52	57.14
Au_8	1749.01	18.86	96.70	76.19

"Schwarz integral screening threshold of 10^{-14} is used in the calculations. The full Gaunt contribution is scaled by 1/2 in the Breit operator.

Quantum software package³¹ with the Dirac-Hartree-Fock (DHF) method using the DCB Hamiltonian. The speed of light utilized in this study is 137.035999074 au. All calculations utilized the standard Gaussian nuclear model.³² The self-consistent-field optimization is done in the Kramers unrestricted framework, where the lowest N_{ε} positive energy orbitals are singly occupied.

The uncontracted ANO-RCC basis^{33–35} set was used in calculations of linear gold chains and potential energy surface scans of Au₂, Ag₂, and Cu₂. To create linear gold chain models, the distance between nearest neighboring gold atoms is fixed at 2.586 Å, which is the equilibrium bond length for Au₂ at the Dirac-Coulomb level of theory.²² This resulted in 297 basis functions per Au atom with up to h orbital angular momentum (24s21p15d11f4g2h).

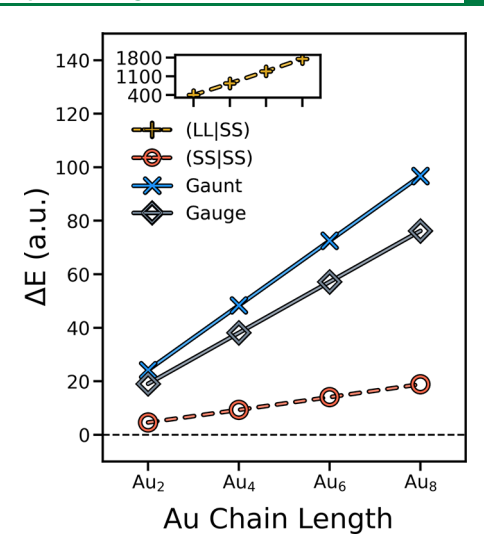


Figure 1. Ground state energy contributions (in au) from the (LLI SS), (SSISS), Gaunt, and gauge terms of the full representation of the DCB operator for linear arrays of gold at two, four, six, and eight atoms in length.

Calculations of metal hexafluorides MF_6 (M = Cr, Mo, W) and tetrahedral lutetium halides LuX_4^- (X = F, Cl, Br, I) used the uncontracted Dyall all-electron 4z basis set. Molecular geometries of MF_6 and LuX_4^- can be found in the Supporting Information.

The uncontracted ANO-RCC-VDZP basis set^{33,39} was used in computational studies of actinyl systems. Linear geometries and experimental bond lengths of 1.76 Å, 1.75 Å, and 1.74 Å were utilized for uranyl, neptunyl, and plutonyl, respectively.⁴⁰

3.2. Locality Analysis of Relativistic Operators. To evaluate the degree of locality of relativistic integrals, we investigate the errors linked to different terms, including (LLI SS), (SSISS), Gaunt, and gauge, in ground state energy calculations of linear gold chains containing two, four, six, and eight atoms. In this analysis, the four-component wave function is optimized by using the full representation of the DCB operator. The energy ΔE^{Term} is obtained by contracting the corresponding relativistic term ((LLISS), (SSISS), Gaunt, or gauge) with the DCB-optimized four-component density matrix.

The results using the full representation of each relativistic term are presented in Table 1 and plotted in Figure 1. Among the four relativistic terms examined in this study, the (LLISS) contribution emerges as the largest, followed by Gaunt and gauge, while the (SSISS) term is found to be the smallest. Consistent with expectations, the energy contributions from all relativistic terms exhibit an upward trend as the system size increases. However, it is noteworthy that the increase in the energy contribution follows a linear pattern in relation to the system size. This observation suggests that the interactions are short-range, which is in agreement with the nature of the operator in the modified Dirac representation, characterized by an r^{-3} or r^{-5} dependence. Furthermore, the four terms demonstrate distinct growth behaviors, indicating different localities associated with the underlying relativistic contributions

To assess the accuracy of various local approximations, we compute the error of each local approximation in relation to the exact calculation:

Table 2. Signed Error (in au) of the (LLISS), (SSISS), Gaunt, and Gauge Terms Using Different Local Approximations (see Supporting Information for Reference Energies Used in This Analysis)^a

	Dirac-Coulomb		Br	Breit		
	(LLISS)	(SSISS) ^b	Gaunt	gauge		
	A1N Approximation					
Au_2	1.6×10^{1} (4.13%)	5.2×10^{-2} (1.14%)	-1.5×10^{-6}	-3.3×10^{-6}		
Au_4	7.1×10^1 (8.49%)	2.3×10^{-1} (2.44%)	4.2×10^{-6}	-5.1×10^{-7}		
Au_6	1.4×10^2 (11.04%)	4.6×10^{-1} (3.24%)	9.3×10^{-6}	2.2×10^{-6}		
Au_8	2.2×10^2 (12.81%)	7.2×10^{-1} (3.82%)	1.4×10^{-5}	5.0×10^{-6}		
	, ,	A2N Approx	rimation			
Au_2	2.4×10^{-1} (0.06%)	1.2×10^{-6}	-1.8×10^{-6}	-3.7×10^{-6}		
Au_4	7.5×10^{-1} (0.09%)	5.2×10^{-6}	3.2×10^{-6}	-1.7×10^{-6}		
Au_6	1.4 × 10 ° (0.11%)	1.1×10^{-5}	7.6×10^{-6}	2.4×10^{-7}		
Au_8	$2.0 \times 10^{\circ}$ (0.12%)	1.7×10^{-5}	1.1×10^{-5}	2.3×10^{-6}		
	SS2N Approximation					
Au_2	2.0×10^{-4}	_	1.4×10^{-6}	2.0×10^{-6}		
Au_4	1.9×10^{-1} (0.02%)	1.3×10^{-6}	7.9×10^{-6}	7.6×10^{-6}		
Au_6	4.9×10^{-1} (0.04%)	3.6×10^{-6}	1.6×10^{-5}	1.4×10^{-5}		
Au_8	8.5×10^{-1} (0.05%)	6.6×10^{-6}	2.5×10^{-5}	2.1×10^{-5}		
SS3N Approximation ^c						
Au_2	2.0×10^{-4}	_	1.4×10^{-6}	2.0×10^{-6}		
Au_4	8.4×10^{-4}	<10 ⁻¹⁰	7.0×10^{-6}	7.3×10^{-6}		
Au_6	1.7×10^{-3}	<10 ⁻¹⁰	1.4×10^{-5}	1.3×10^{-5}		
Au_8	2.6×10^{-3}	<10 ⁻¹⁰	2.0×10^{-5}	1.9×10^{-5}		

^aPercent error is computed as $\frac{\delta E_{A\rm nN}^{\rm Term}}{\Delta E_{\rm full}^{\rm Term}}$. Only percent errors that are greater than 0.01% are shown in parenthesis. Schwarz integral screening threshold of 10^{-14} is used in the calculations. ^bThe SS2N and SS3N approaches are exact for the (SSISS) term of Au₂. ^cThe numerical errors using the SS3N approximation for the (SSISS) term are below the SCF convergence.

$$\delta E_{\rm approx}^{\rm Term} = \Delta E_{\rm full}^{\rm Term} - \Delta E_{\rm approx}^{\rm Term}$$

Term $\in \{(LL|SS), (SS|SS), Gaunt, gauge\}$

where $\Delta E_{\mathrm{approx}}^{\mathrm{Term}}$ is the energy for the local approximation and 'full' is exact without any local approximations. $\Delta E_{\mathrm{approx}}^{\mathrm{Term}}$ is computed by directly contracting local integrals with the exact four-component density matrix, resulting from the calculation using the full DCB operator. The errors for relativistic terms are tabulated in Table 2 and plotted in Figure 2 for linear gold chains with two, four, six, and eight atoms.

3.2.1. Locality of the Dirac-Coulomb Terms. In Table 2, we can observe the impact of the A2N integral approximation on the (LLISS) term, revealing significant absolute errors in the range of \sim 0.2–2 a.u. Despite these notable absolute errors, the percent error relative to the full (LLISS) energy contribution remains small (<0.12%). In contrast, the (SSISS) A2N approximation demonstrates excellent error control, with absolute errors ranging from 10^{-5} to 10^{-6} a.u. and percent errors below 0.01%.

The error in the Dirac-Coulomb terms increases significantly when the A1N approximation is employed, exhibiting percent errors of 12.81% and 3.82% for (LLISS) and (SSISS), respectively, in the Au_8 system.

When the restriction is relaxed in the SS3N and SS2N approximations for the large-component of the (LLISS) term, the absolute error is significantly improved to 10^{-4} to 10^{-1} a.u. (<0.05% percent error). This observation suggests that the leading error in local (LLISS) approximations comes from forcing the locality of the large-component density. However, the SS2N approximation only marginally improves the absolute error associated with the (SSISS) term, suggesting that A2N approximation captures the leading contribution to the total energy. When the SS3N approximation is employed for the (SSISS) term, the error falls below the convergence criterion. This observation indicates that the contribution from four-center (SSISS) integrals is essentially zero.

The Dirac-Coulomb operator plays a crucial role as the leading relativistic contribution with (LLISS) representing the interaction between the large and small components of the system. Additionally, it is important to note that Coulombic repulsion between internuclear small components arising from the (SSISS) term is crucial for accurate description of the bond length between multiple late-row elements. The error analysis shown in Table 2 suggests that both the (LLISS) and (SSISS) contributions are nonlocal. More specifically, the SS charge densities can be treated as local, but these densities can be on different centers. The LL charge densities cannot be treated as local. When there are multiple late-row elements, employing drastic local approximations will lead to a significant error in energy.

3.2.2. Locality of the Breit Terms. In Table 2, we observe that all of the local approximations maintain a small error for both the Gaunt and gauge term in the Breit operator, without any significant reduction in its accuracy. The error in both terms is much smaller than those found in the terms of the Dirac-Coulomb operator. Figure 2 shows that the error from all local approximations remains small throughout the whole series, on the order of 10^{-5} to 10^{-7} au, thereby indicating the high locality of the Gaunt and gauge terms. A comparative analysis of all four local approximations reveals that the highly localized approach, the A1N approximation, performs well in capturing the majority of the energy contribution stemming from the Breit operator.

The two distinct local approximations exhibit somewhat different behaviors for the Breit operator. The comparison of the local atomic A2N method with the local small-component SS2N approach yields notable insights, especially since both operate on an $O(N)^2$ algorithmic scale, where N is the number of atoms. The A2N approximation enforces the atomic locality of the current densities in the integrals, whereas the SS2N approximation enforces the locality of small components. The larger errors in SS2N can be attributed to the exclusion of integrals, in which both current densities in an integral are localized but on different atoms. Thus the locality of the current densities in an integral is the most important consideration, rather than the locality of the small components.

3.3. Atomic Breit Approximations. By selectively exploiting the locality of the current densities in the Breit integrals, an accurate low-scaling approximation can be built for molecular systems. Data from the previous section have shown that applying local approximations drastically reduces the cost for every term in the DCB operator, but the accuracy

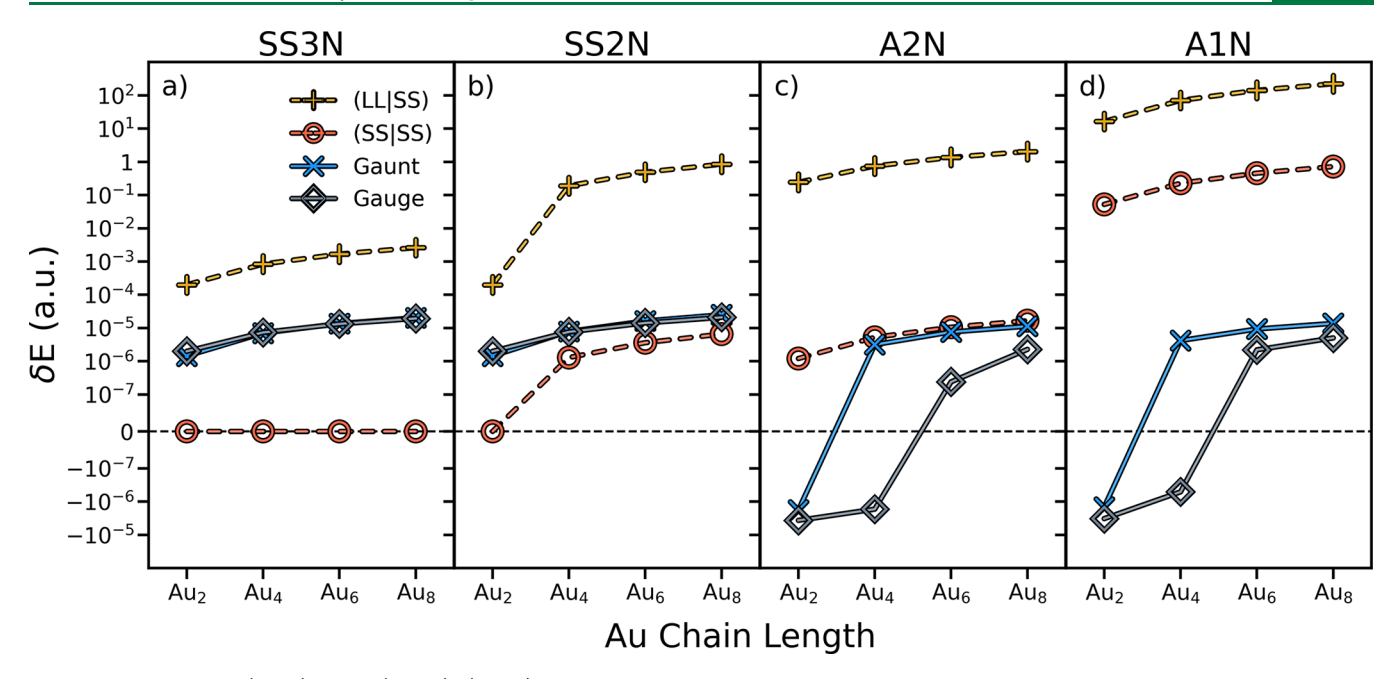


Figure 2. Signed error (in au) of the (LLISS), (SSISS), Gaunt, and gauge terms using local relativistic integral approximations for linear arrays of gold at two, four, six, and eight atoms in length. Panel (a) shows the SS3N approximation, (b) the SS2N approximation, (c) the A2N approximation, and (d) the A1N approximation.

Table 3. Ground State Energy of Transition Metal Hexafluorides Computed Using the Atomic Breit Hamiltonian and the Full DCB Operator in a.u.^a

	CrF_6	MoF_6	WF_6
DC* ^b + Atomic Breit	-1646.4864201592	-4642.4027360282	-16736.8599690070
Full DCB	-1646.4859527919	-4642.4023005053	-16736.8595610761
Absolute Error	4.7×10^{-4}	4.4×10^{-4}	4.1×10^{-4}
% Error	2.8×10^{-5}	9.4×10^{-6}	2.4×10^{-6}

^aThe symmetry of the molecules was restricted to O_h . Absolute error (a.u.) is the unsigned difference between the two ground state energies. Percent error is defined with respect to the full DCB result. ^bDC* uses the full (LL|SS) expression with the A2N approximation for the (SS|SS) term.

Table 4. Metal 2p and Valence t_{2g} Orbital Fine Structure Splitting of Transition Metal Hexafluorides Computed Using the Atomic Breit Hamiltonian and the Full DCB operator in a.u.^a

	CrF ₆	MoF_6	WF ₆	
	Metal	2 <i>p</i>		
DC* ^b + Atomic Breit	0.3148801509	3.8779210220	49.2697066779	
Full DCB	0.3148798716	3.8779209607	49.2697062763	
Absolute Error	2.8×10^{-7}	6.1×10^{-8}	4.0×10^{-7}	
% Error	8.9×10^{-5}	1.6×10^{-6}	8.2×10^{-7}	
Valence t_{2g}				
DC*+ Atomic Breit	0.0022743010	0.0054973971	0.0181564393	
Full DCB	0.0022791956	0.0055038072	0.0181641239	
Absolute Error	4.9×10^{-6}	6.4×10^{-6}	7.7×10^{-6}	
% Error	2.1×10^{-1}	1.2×10^{-1}	4.2×10^{-2}	

^aAll molecules were restricted to O_h symmetry. Absolute error (a.u.) is the unsigned difference between the two results. Percent error is defined with respect to the full DCB result. ^bDC* uses the full (LLI SS) expression with A2N approximation for the (SSISS) term.

loss can differ substantially between each term. In this section, we propose an approximation scheme that minimizes the computational cost while maintaining a high level of accuracy. Our proposed approximation uses the least expensive local

approximation for each term that is accurate to the order of $\sim 1 \times 10^{-4}$ a.u. (~ 2.7 meV). The approximation is as follows:

$$\mathbf{H} = \mathbf{H}^{\mathrm{DC}^*} + \mathbf{H}^{\mathrm{Breit}}_{\mathrm{A1N}} \tag{3}$$

where H^{DC*} uses the full (LLISS) integral set with the A2N approximation for the (SSISS) term. We opted to utilize the full (LLISS) set despite the SS3N approach offering reasonable accuracy. This decision is primarily motivated by the fact that the computational savings achieved by the SS3N approach are relatively marginal, amounting to less than 10%. This minor reduction is largely attributable to the effective screening out of a majority of the four-center integrals, which means that the computational advantage does not sufficiently outweigh the benefits of utilizing the full (LLISS) integral set. Since the Breit term (including both Gaunt and gauge contributions) is purely atomic, the proposed Hamiltonian will be called the atomic Breit Hamiltonian.

We tested the accuracy of the atomic Breit Hamiltonian on a series of octahedral metal hexafluorides MF₆ (M = Cr, Mo, W) and tetrahedral lutetium halides LuX₄ (X = F, Cl, Br, I). Table 3 tabulates the atomic Breit and DCB ground state energies of MF₆. The metal center was varied to show that the approximation can closely reproduce DCB results at various strengths of relativistic effects. The atomic Breit Hamiltonian consistently recovers the DCB energy within $\sim \! 5 \times 10^{-4}$ a.u.

Table 5. Ground State Energy of LuX $_{-}^{-}$ (X = F, Cl, Br, I) Computed Using the Atomic Breit Hamiltonian and the Full DCB Operator in a.u. The symmetry of the molecules was restricted to T_d^a

	LuF ₄	LuCl ₄	LuBr ₄	LuI_4^-
DC* ^b + Atomic Breit	-14956.0830329282	-16401.6882791474	-24972.9613856172	-42999.7316668137
Full DCB	-14956.0829646465	-16401.6882485021	-24972.9614276801	-42999.7316404461
Absolute Error	6.8×10^{-5}	3.0×10^{-5}	4.2×10^{-5}	2.6×10^{-5}
% Error	4.6×10^{-7}	1.9×10^{-7}	1.7×10^{-7}	6.1×10^{-8}

[&]quot;Absolute error (a.u.) is the unsigned difference between the two ground state energies. Percent error is defined with respect to the full DCB result. bDC* uses the full (LLISS) expression with A2N approximation for the (SSISS) term.

Table 6. Lu 2p and t_2 (4d) Orbital Fine Structure Splitting of LuX₄⁻ (X = F, Cl, Br, I) Computed Using the Atomic Breit Hamiltonian and the Full DCB Operator in a.u.^a

		LuF ₄	LuCl ₄	LuBr ₄	LuI_4^-
2 <i>p</i>	DC* ^b + Atomic Breit	40.7028738070	40.7035398838	40.7032207043	40.7036328291
	Full DCB	40.7028731375	40.7035398482	40.7032202084	40.7036327990
	Absolute Error	6.7×10^{-7}	3.6×10^{-8}	5.0×10^{-7}	3.0×10^{-8}
	% Error	1.6×10^{-6}	8.7×10^{-8}	1.2×10^{-6}	7.4×10^{-8}
$4d(\Gamma_1 - \Gamma_2)$	DC*+ Atomic Breit	0.3754660414	0.3751800128	0.3755814913	0.3753164491
splitting	Full DCB	0.3754601634	0.3751772965	0.3755761608	0.3753132647
	Absolute Error	5.9×10^{-6}	2.7×10^{-6}	5.3×10^{-6}	3.2×10^{-6}
	% Error	1.6×10^{-3}	7.2×10^{-4}	1.4×10^{-3}	8.5×10^{-4}
$4d(\Gamma_2 - \Gamma_3)$	DC*+ Atomic Breit	0.0004421744	0.0001117709	0.0002022306	0.0000734257
splitting	Full DCB	0.0004428107	0.0001121452	0.0002028300	0.0000738457
	Absolute Error	6.4×10^{-7}	3.7×10^{-7}	6.0×10^{-7}	4.2×10^{-7}
	% Error	1.4×10^{-1}	3.3×10^{-1}	3.0×10^{-1}	5.7×10^{-1}

^aMolecules were restricted to T_d symmetry. Absolute error (a.u.) is the unsigned difference between the two results. Percent error is defined with respect to the full DCB result. ^bDC* uses the full (LLISS) expression with A2N approximation for the (SSISS) term.

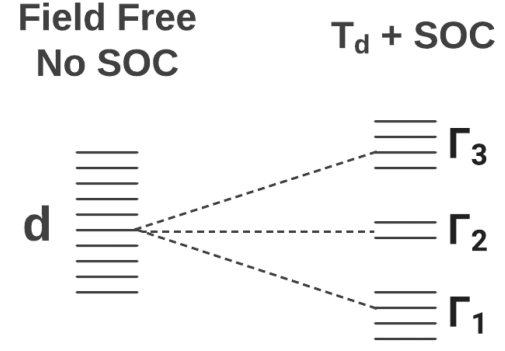


Figure 3. Splitting of d orbitals in a T_d ligand field with spin—orbit coupling. Each line represents one spin—orbital. Degenerate spin—orbitals are grouped under irreducible representations Γ_n .

(~14 meV), below the chemical accuracy. The error remained on the same order of magnitude when increasing the atomic number of the metal. This shows that the atomic Breit Hamiltonian is insensitive to the atomic number. Percent errors are greater for light molecules because their ground state energy tends to be lower in magnitude while the atomic Breit error remains relatively constant.

The hallmark of the DCB operator is its ability to capture the relativistic spin physics. The assessment of the atomic Breit Hamiltonian would be incomplete without a benchmark of spin-derived quantities. Hence, the accuracy was also tested by comparing the orbital fine structure splitting of MF₆. Table 4 shows the fine structure splitting of the MF₆ metal 2p and valence t_{2g} orbitals. Errors remained on a similar order of magnitude with increasing atomic number for both sets of orbitals. Errors were slightly higher for the valence t_{2g} . This is possibly due to stronger interatomic electron interaction in t_{2g}

Table 7. Ground State SCF Energies of Three Actinyls Computed Using the Atomic Breit Hamiltonian and the Full DCB Operator in a.u.^a

_		
Uranyl (UO_2^{2+})	DC*+ Atomic Breit	-28164.7164285082
	Full DCB	-28164.7162599324
	Absolute Error	1.7×10^{-4}
	% Error	6.0×10^{-7}
Neptunyl (NpO_2^{2+})	DC*+ Atomic Breit	-28957.3138968723
	Full DCB	-28957.3137395559
	Absolute Error	1.6×10^{-4}
	% Error	5.4×10^{-7}
Plutonyl (PuO ₂ ²⁺)	DC*+ Atomic Breit	-29765.3077511379
	Full DCB	-29765.3076211330
	Absolute Error	1.3×10^{-4}
	% Error	4.4×10^{-7}

[&]quot;Absolute error (au) is the unsigned difference between the two results. Percent error is defined with respect to the full DCB result.

Table 8. Cost Comparison of the Full $(T_{\rm full})$ and Atomic $(T_{\rm atomic})$ Dirac-Coulomb-Breit Hamiltonian, Where $T_{\rm full}$ and $T_{\rm atomic}$ Are the CPU Times to Build the Four-Component Fock Matrix in the Pauli Quaternion Basis^a

Molecule	$T_{ m full}/T_{ m atomic}$
$\mathrm{LuBr_4^{-1}}$	6.7
LuI_4^{-1}	6.5
MoF_6	9.8
WF_6	9.3

"Schwarz integral screening threshold of 10^{-14} is used in the calculations. In the atomic Dirac-Coulomb-Breit Hamiltonian, the Dirac-Coulomb term uses the full (LLISS) expression with A2N approximation for the (SSISS) term.

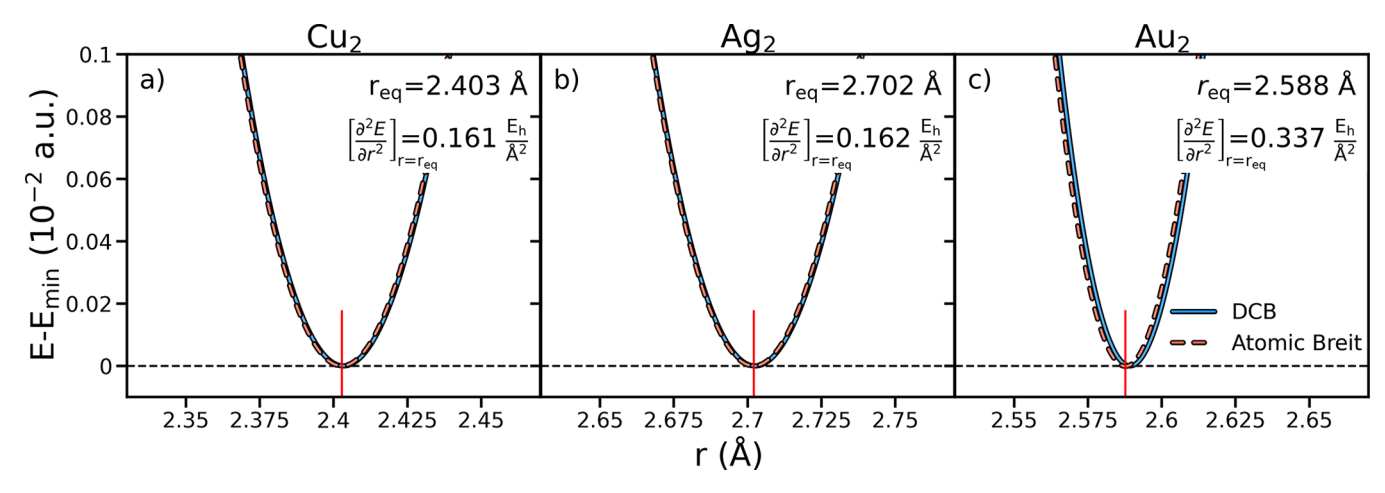


Figure 4. Potential energy surfaces of the Cu, Ag, and Au dimers computed using the atomic Breit and full DCB Hamiltonians. The equilibrium distance and second derivative at the minimum of the atomic Breit Hamiltonian are shown in the corresponding panels. The minimum position is marked with a red vertical line.

where there is significant mixing between ligand and metal orbitals. Nevertheless, the errors are well below $\sim 10^{-5}$ au.

The MF₆ series only tests the accuracy of the atomic Breit Hamiltonian for varying strengths of relativistic effects for one atom. Because interatomic electron interactions are approximated in the local approximations, we must assess the accuracy of the atomic Breit Hamiltonian for varying atomic numbers in ligands as well. For this, we turn to tetrahedral LuX_4^- (X = F, Cl, Br, I). Table 5 shows the atomic Breit and DCB ground state energies for LuX₄⁻. Similar to MF₆, the LuX₄⁻ errors were well within chemical accuracy and remained on the same order of magnitude with varying ligand atomic number. Table 6 shows the orbital fine structure splitting of LuX₄ metal 2p and metal 4d orbitals. The semicore position of the 4d orbitals means that it experiences significant spin-orbit coupling while being mostly shielded from the ligand field. However, a small but non-negligible amount of ligand field splitting is still observed in the 4d orbitals. Figure 3 shows how the 4d orbitals split under both spin-orbit coupling and a T_d ligand field. The error for both 2p and 4d orbitals were also well within spectroscopic accuracy and remained on a similar order of magnitude for varying ligand atomic number.

Although the relative error of the atomic Breit approximation is small in the benchmark studies using closed-shell transition metal and rare earth complexes, its accuracy on open-shell systems with a strong relativistic effect needs to be tested. As such, we also analyze the accuracy of the atomic Breit Hamiltonian for open-shell systems consisting of heavy elements. Table 7 compares the computed total energies of early actinyl molecules including open-shell NpO $_2^{2+}$ and PuO $_2^{2+}$ complexes. The results show that the absolute error of the atomic Breit Hamiltonian remains small, on the order of 10^{-4} a.u. There is no significant difference in the absolute error between the closed-shell UO $_2^{2+}$ molecule and open-shell NpO $_2^{2+}$ and PuO $_2^{2+}$ complexes.

Table 8 shows the relative speed-up factor for building the four-component Fock matrix using the atomic Breit Hamiltonian as compared with using the full Hamiltonian. The atomic Breit Hamiltonian exhibits an impressive 6 to 10-fold speed-up without compromising accuracy. As the number of nearest-neighbor atomic pairs increases, the speed-up also increases. This is understandable because the nearest-neighbor interactions are not subject to Schwarz screening, and thus the

effectiveness of the atomic Breit approximation becomes more pronounced.

Finally, the potential energy surface (PES) of the Cu, Ag, and Au dimers around their local minima is plotted in Figure 4. The data give insight into the spectroscopic properties of the group 11 atomic dimers. A fourth order polynomial is fit to the data to calculate the equilibrium interatomic distance as well as the second derivative at the minimum. PESs computed using atomic Breit and full DCB Hamiltonians are indistinguishable. The harmonic vibrational frequencies at the minimum energy can be obtained from the second derivative of the PES. These values are 194.842 cm⁻¹ for Cu₂, 149.625 cm⁻¹ for Ag₂, and 159.175 cm⁻¹ for Au₂. The corresponding vibrational frequencies for the full DCB operator are 195.007 cm⁻¹ for Cu₂, 149.431 cm⁻¹ for Ag₂, and 159.255 cm⁻¹ for Au₂. This indicates that the atomic Breit Hamiltonian can recover the vibrational frequencies of these systems to within ~0.2 cm⁻¹ of the full DCB representation.

4. CONCLUSION AND PERSPECTIVES

The DCB operator represents state-of-the-art in its ability to capture relativistic effects and spin physics for molecular systems. In this study, we presented an assessment of the locality of integral contributions to the Fock matrix arising from the DCB operator, using a set of low-scaling local relativistic integral approximations, and investigated the errors linked to the individual (LLISS), (SSISS), Gaunt, and gauge terms in ground state energy calculations of linear gold chains. Using the full calculation of all the terms, the linear trend in energetic contributions from each term as a function of system size suggested that the interactions are short-range in nature. In order to establish a connection between these results and the locality of the relativistic integral contributions, the error of each local approximation was computed relative to the exact calculation for each term. These approximations selectively screen out integrals, keeping only terms where electronelectron interactions are localized to single atoms (A1N) or pairs of atoms (A2N), or localized to small-component densities (SS2N or SS3N). Our observations suggest that the Gaunt and gauge terms are very local in nature, where most of the energy is captured by the A1N approximation. The (LLI SS) and (SSISS) terms on the other hand rely on more

nonlocal interactions and need at least an SS2N representation to accurately capture the energy.

These results inform the formulation of the atomic Breit Hamiltonian, whereby by selectively exploiting the locality of individual terms of the DCB operator, an accurate yet low-scaling Hamiltonian can be built for molecular systems. Benchmark studies on the atomic Breit approximation demonstrated that this approximation can recover the energy with remarkable accuracy, to within 1 kcal/mol ($\sim 10^{-4}$ a.u.) of the full DCB operator. In addition, the atomic Breit Hamiltonian exhibits an impressive 6 to 10-fold speed-up as compared to using the full Hamiltonian. Note that in a recent parallel work, Quiney and co-workers reached a similar conclusion regarding the locality of the Breit Hamiltonian.

Moving forward, we believe that future developments in the relativistic electronic structure theory should exploit the local nature of certain relativistic interactions. In particular, the locality analysis presented herein should serve as a template for the formulation and development of accurate, yet efficient, implementations of relativistic operators.

ASSOCIATED CONTENT

Supporting Information

The Supporting Information is available free of charge at https://pubs.acs.org/doi/10.1021/acs.jctc.3c01012.

Molecular structures (PDF)

AUTHOR INFORMATION

Corresponding Author

Xiaosong Li — Department of Chemistry, University of Washington, Seattle, Washington 98195, United States; orcid.org/0000-0001-7341-6240; Email: xsli@uw.edu

Authors

Can Liao – Department of Chemistry, University of Washington, Seattle, Washington 98195, United States Eleftherios Lambros – Department of Chemistry, University of Washington, Seattle, Washington 98195, United States Qiming Sun – AxiomQuant Investment Management LLC, Shanghai 200120, China

Kenneth G. Dyall – Dirac Solutions, Portland, Oregon 97229, United States; orcid.org/0000-0002-5682-3132

Complete contact information is available at: https://pubs.acs.org/10.1021/acs.jctc.3c01012

Author Contributions

*C.L. and E.L. contributed equally.

Notes

The authors declare no competing financial interest.

■ ACKNOWLEDGMENTS

This work is supported by the U.S. Department of Energy, Office of Science, Basic Energy Sciences, in the Computational and Theoretical program (Grant No. DE-SC0006863) for the development of the Breit operator for Dirac and quantum field theory. The development of the Chronus Quantum computational software is supported by the Office of Advanced Cyberinfrastructure, National Science Foundation (Grant No. OAC-2103717). Computations were facilitated through the use of advanced computational, storage, and networking infrastructure provided by the shared facility supported by

the University of Washington Molecular Engineering Materials Center (DMR-1719797) via the Hyak supercomputer system.

REFERENCES

- (1) Grant, I. P.; Penney, W. G. Relativistic Self-Consistent Fields. *Proc. R. Soc. London, Ser. A* **1961**, 262, 555–576.
- (2) Mann, J. B.; Johnson, W. R. Breit Interaction in Multielectron Atoms. *Phys. Rev. A* 1971, 4, 41–51.
- (3) Huang, K.-N.; Aoyagi, M.; Chen, M. H.; Crasemann, B.; Mark, H. Neutral-atom Electron Binding energies from Relaxed-orbital Relativistic Hartree-Fock-Slater Calculations $2 \le Z \le 106$. Atomic Data and Nuclear Data Tables 1976, 18, 243–291.
- (4) Lindroth, E.; Martensson-Pendrill, A.-M.; Ynnerman, A.; Oster, P. Self-Consistent Treatment of the Breit Interaction, with Application to the Electric Dipole Moment in Thallium. *J. Phys. B* **1989**, 22, 2447–2464.
- (5) Eliav, E.; Kaldor, U.; Ishikawa, Y. Open-Shell Relativistic Coupled-Cluster Method with Dirac-Fock-Breit Wave Functions: Energies of the Gold Atom and its Cation. *Phys. Rev. A* **1994**, *49*, 1724–1729.
- (6) Ishikawa, Y.; Koc, K. Relativistic Many-Body Perturbation Theory Based on the No-Pair Dirac-Coulomb-Breit Hamiltonian Relativistic Correlation Energies for the Noble-Gas Sequence through Rn (Z = 86), the Group-IIB Atoms through Hg, and the Ions of Ne Isoelectronic Sequence. *Phys. Rev. A* **1994**, *50*, 4733–4742.
- (7) Vilkas, M.; Ishikawa, Y.; Hirao, K. Ionization Energies and Fine Structure Splittings of Highly Correlated Systems: Zn, Zinc-like Ions and Copper-like Ions. *Chem. Phys. Lett.* **2000**, *321*, 243–252.
- (8) Grant, I. P.; Quiney, H. M. Application of Relativistic Theories and Quantum Electrodynamics to Chemical Problems. *Int. J. Quantum Chem.* **2000**, *80*, 283–297.
- (9) Chantler, C. T.; Nguyen, T. V. B.; Lowe, J. A.; Grant, I. P. Convergence of the Breit Interaction in Self-consistent and Configuration-interaction Approaches. *Phys. Rev. A* **2014**, *90*, No. 062504.
- (10) Kozioł, K.; Giménez, C. A.; Aucar, G. A. Breit Corrections to Individual Atomic and Molecular Orbital Energies. *J. Chem. Phys.* **2018**, *148*, No. 044113.
- (11) Liu, W. Essentials of Relativistic Quantum Chemistry. J. Chem. Phys. 2020, 152, No. 180901.
- (12) Zhang, C.; Cheng, L. Atomic Mean-Field Approach within Exact Two-Component Theory Based on the Dirac—Coulomb—Breit Hamiltonian. *J. Phys. Chem. A* **2022**, *126*, 4537—4553.
- (13) Dyall, K. G.; Fægri, K, Jr Introduction to Relativistic Quantum Chemistry; Oxford University Press, 2007.
- (14) Reiher, M.; Wolf, A. Relativistic Quantum Chemistry, 2nd ed.; Wiley-VCH, 2015.
- (15) Grant, I. P. Relativistic Quantum Theory of Atoms and Molecules: Theory and Computation; Springer Science & Business Media, 2007; Vol. 40.
- (16) Lindgren, I. Relativistic Many-Body Theory: A New Field-Theoretical Approach; Springer: Switzerland, 2016.
- (17) Thierfelder, C.; Schwerdtfeger, P. Quantum Electrodynamic Corrections for the Valence Shell in Heavy Many-electron Atoms. *Phys. Rev. A* **2010**, 82, No. 062503.
- (18) Pyykkö, P. The Physics behind Chemistry and the Periodic Table. Chem. Rev. 2012, 112, 371–384.
- (19) Pyykkö, P. Relativistic Effects in Chemistry: More Common Than You Thought. *Annu. Rev. Phys. Chem.* **2012**, *63*, 45–64.
- (20) Liu, W., Lindgren, I. Going beyond "No-pair Relativistic Quantum Chemistry". *J. Chem. Phys.* **2013**, *139*, No. 014108.
- (21) Liu, W. Advances in Relativistic Molecular Quantum Mechanics. *Phys. Rep.* **2014**, *537*, 59–89.
- (22) Sun, S.; Stetina, T. F.; Zhang, T.; Hu, H.; Valeev, E. F.; Sun, Q.; Li, X. Efficient Four-Component Dirac-Coulomb-Gaunt Hartree-Fock in the Pauli Spinor Representation. *J. Chem. Theory Comput.* **2021**, *17*, 3388–3402.

- (23) Sun, S.; Ehrman, J. N.; Sun, Q.; Li, X. Efficient Evaluation of the Breit Operator in the Pauli Spinor Basis. *J. Chem. Phys.* **2022**, *157*, No. 064112.
- (24) Breit, G. Dirac's Equation and the Spin-Spin Interaction of Two Electrons. *Phys. Rev.* **1932**, *39*, 616–624.
- (25) Shiozaki, T. Communication: An Efficient Algorithm for Evaluating the Breit and Spin-Spin Coupling Integrals. *J. Chem. Phys.* **2013**, *138*, No. 111101.
- (26) Kelley, M. S.; Shiozaki, T. Large-Scale Dirac-Fock-Breit Method Using Density Fitting and 2-Spinor Basis Functions. *J. Chem. Phys.* **2013**, *138*, No. 204113.
- (27) Dyall, K. G. An Exact Separation of the Spin-Free and Spin-Dependent Terms of the Dirac-Coulomb-Breit Hamiltonian. *J. Chem. Phys.* **1994**, *100*, 2118–2127.
- (28) Sun, S.; Ehrman, J.; Zhang, T.; Sun, Q.; Dyall, K. G.; Li, X. Scalar Breit Interaction for Molecular Calculations. *J. Chem. Phys.* **2023**, *158*, No. 171101.
- (29) Dyall, K. G.; Fægri, J. K. Introduction to Relativistic Quantum Chemistry; Oxford University Press: New York, 2007; Chapter 11.
- (30) Heß, B. A.; Marian, C. M.; Wahlgren, U.; Gropen, O. A Mean-Field Spin-Orbit Method Applicable to Correlated Wavefunctions. *J. Chem. Phys.* **1996**, *251*, 365–371.
- (31) Williams-Young, D. B.; Petrone, A.; Sun, S.; Stetina, T. F.; Lestrange, P.; Hoyer, C. E.; Nascimento, D. R.; Koulias, L.; Wildman, A.; Kasper, J.; Goings, J. J.; Ding, F.; DePrince, A. E., III; Valeev, E. F.; Li, X. The Chronus Quantum (ChronusQ) Software Package. WIREs Comput. Mol. Sci. 2020, 10, No. e1436.
- (32) Visscher, L.; Dyall, K. Dirac-Fock Atomic Electronic Structure Calculations using Different Nuclear Charge Distributions. *Atomic Data and Nuclear Data Tables* 1997, 67, 207–224.
- (33) Roos, B. O.; Lindh, R.; Malmqvist, P.-Å.; Veryazov, V.; Widmark, P.-O. Main Group Atoms and Dimers Studied with a New Relativistic ANO Basis Set. *J. Phys. Chem. A* **2004**, *108*, 2851–2858.
- (34) Roos, B. O.; Lindh, R.; Malmqvist, P.-Å.; Veryazov, V.; Widmark, P.-O. New Relativistic ANO Basis Sets for Transition Metal Atoms. *J. Phys. Chem. A* **2005**, *109*, 6575–6579.
- (35) Roos, B. O.; Lindh, R.; Malmqvist, P.-Å.; Veryazov, V.; Widmark, P.-O.; Borin, A. C. New Relativistic Atomic Natural Orbital Basis Sets for Lanthanide Atoms with Applications to the Ce Diatom and LuF₃. *J. Phys. Chem. A* **2008**, *112*, 11431–11435.
- (36) Dyall, K. G. Relativistic Double-Zeta, Triple-Zeta, and Quadruple-Zeta Basis Sets for the 5d Elements Hf Hg. *Theor. Chem. Acc.* **2004**, *112*, 403–409.
- (37) Dyall, K. G. Relativistic Double-Zeta, Triple-Zeta, and Quadruple-Zeta Basis Sets for the 4d Elements Y Cd. *Theor. Chem. Acc.* **2007**, *117*, 483–489.
- (38) Dyall, K. G. Relativistic Double-Zeta, Triple-Zeta, and Quadruple-Zeta Basis Sets for the Light Elements H Ar. *Theor. Chem. Acc.* **2016**, *135*, 128.
- (39) Roos, B. O.; Lindh, R.; Malmqvist, P.-A.; Veryazov, V.; Widmark, P.-O. New Relativistic ANO Basis Sets for Actinide Atoms. *Chem. Phys. Lett.* **2005**, *409*, 295–299.
- (40) Sergentu, D.; Duignan, T.; Autschbach, J. Ab initio Study of Covalency in the Ground versus Core-Excited States and X-ray Absorption Spectra of Actinide Complexes. J. Phys. Chem. Lett. 2018, 9, 5583–5591.
- (41) Visscher, L. Approximate Molecular Relativistic Dirac-Coulomb Calculations Using a Simple Coulombic Correction. *Theor. Chem. Acc.* **1997**, *98*, *68*–70.
- (42) Flynn, D. J.; Grant, I. P.; Quiney, H. M. Nuclear Structure and Breit Interaction Effects in Relativistic Molecular Electronic Structure Calculations. *Mol. Phys.* **2023**, No. e2262610.